Tuning odd triplet superconductivity by spin pumping

Takehito Yokoyama[1] and Yaroslav Tserkovnyak[2]
[1]*Department of Applied Physics, University of Tokyo, Tokyo 113-8656, Japan*
[2]*Department of Physics and Astronomy, University of California, Los Angeles, California 90095, USA*
(Received 24 June 2009; revised manuscript received 7 August 2009; published 14 September 2009)

We study proximity effect in diffusive ferromagnet/normal-metal/superconductor junction with precessing magnetization of the ferromagnet. We find that the odd-frequency pairing induced in the normal metal is modified by spin pumping from the ferromagnet and hence can be tuned by changing the precessional frequency. At the frequency corresponding to twice the superconducting gap, the odd-frequency pairing is strongly enhanced. We find that the odd-frequency pairing can be dominant over the even-frequency pairing in the normal metal by tuning the precessional frequency. This gives a clearcut signature of the odd-frequency superconductivity observable by scanning-tunneling microscopy. According to the pairing symmetries in the normal metal, we find a crossover from the gap to the peak structure in the tunneling conductance between the normal metal and a scanning-tunneling microscope tip.

DOI: 10.1103/PhysRevB.80.104416 PACS number(s): 75.75.+a, 73.20.−r, 75.50.Xx, 75.70.Cn

I. INTRODUCTION

Generally, superconducting correlations can be even or odd in frequency depending on their symmetry with respect to the time axis. In accordance with the fermionic statistics, even-frequency superconductors are characterized by the spin-singlet even-parity or spin-triplet odd-parity pairing states, while odd-frequency superconductors are grouped into the spin-singlet odd-parity or spin-triplet even-parity pairing states.

The possibility of the odd-frequency pairing state in a uniform system was discussed in the literature[1–5] although its realization in bulk materials is still controversial. The odd-frequency pairing state has recently been predicted in inhomogeneous superconducting systems.[6–13] In diffusive ferromagnet/superconductor junctions, odd-frequency pairings emerge due to the broken symmetry in spin space.[6,7] In the dirty limit, only *s*-wave symmetry of the pair amplitude can survive impurity scattering and hence triplet pairing inevitably belongs to the odd-frequency superconductivity, which is also called *odd triplet superconductivity*.

Recently, the interplay between ferromagnetism and superconductivity in ferromagnet/normal-metal/superconductor (F/N/S) junctions has been studied using spin-active boundary condition.[14] Another recent progress is the study of the Josephson effect in S/F/S junctions, where it has been established that the ferromagnetic spin dynamics play a crucial role.[15–17] The F/N/S proximity effect in the presence of spin dynamics, however, still remains to be fully understood. Moreover, although the long-range proximity effect by the generation of the odd-frequency triplet pairing has been observed in recent experiments,[18,19] no experiment has succeeded in controlling the magnitude of the odd-frequency pairing to this date.

In this paper, we propose an experimental setup which makes it possible to tune the magnitude of the odd-frequency pairing. We study the proximity effect in diffusive F/N/S junctions with precessing magnetization of the F layer. We find that the odd-frequency pairing induced in the N layer is modified by spin pumping from the F and therefore can be tuned by changing the precessional frequency. At the resonance frequency (i.e., twice the superconducting gap), the odd-frequency pairing is strongly enhanced. We find that the odd-frequency pairing can be dominant over the even-frequency pairing in the N by tuning the precessional frequency. This is reflected in the tunneling conductance between the normal metal and the scanning-tunneling microscope (STM) tip as a crossover from the gap to the peak structure.

II. FORMULATION

We consider a diffusive F/N/S junction with precessing magnetization of the F as shown in Fig. 1. The F/N interface is located at $x=0$ while the N/S interface is at $x=L$. The spin relaxation in the junction is assumed to be weak. Then, a spin density is pumped into the N from F (Ref. 20) while the superconductivity is induced in the N by the proximity effect. Therefore, we can study the interplay between ferromagnetism and superconductivity in the N layer.[14]

Let us take the time-dependent exchange field in the F to be directed along

$$\mathbf{m}(t) = (\sin\theta\cos\Omega t, \sin\theta\sin\Omega t, \cos\theta). \tag{1}$$

Here, Ω is the precessional frequency around z axis and θ is a constant tilt angle. In the rotating frame, such precession

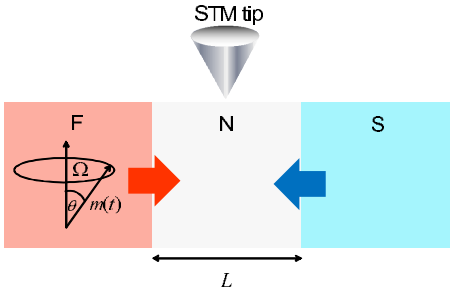

FIG. 1. (Color online) Schematic of the model for a F/N/S junction with precessing magnetization of the F layer. A fictitious exchange field is dynamically induced in the N layer, which interplays with the superconductivity induced by the proximity effect. The electronic structure in the N layer can be studied by STM.

can be viewed as a difference between spin-resolved chemical potentials along the z axis, and the noncollinear effective Zeeman fields in N and F can generate a long-range proximity effect.[16,21,22] To investigate the proximity effect, we use the unitary transformation

$$\hat{g}(t,t') \to U^{\dagger}(t)\hat{g}(t,t')U(t'), \tag{2}$$

where $U(t)=\exp(-i\Omega t\sigma_3/2)$ transforms from the laboratory into the spin-rotating frame. Then, the problem reduces to the stationary one.[16] In fact, we have $U^{\dagger}(t)\mathbf{m}(t)\cdot\boldsymbol{\sigma}U(t)=\mathbf{m}(0)\cdot\boldsymbol{\sigma}\equiv\mathbf{m}\cdot\boldsymbol{\sigma}$. Here, $\hat{g}$ is the retarded component of the quasiclassical Green's function, which is 4×4 matrix in spin $\otimes$ Nambu space. We parameterize $\hat{g}$ as

$$\hat{g}=\tau_3\otimes(g+\mathbf{g}\cdot\boldsymbol{\sigma})+\tau_1\otimes(f_s+\mathbf{f}_t\cdot\boldsymbol{\sigma}), \tag{3}$$

where g and f_s are scalars, and $\mathbf{g}$ and $\mathbf{f}_t$ are three-dimensional vectors.[23] σ_i and τ_i $(i=0,1,2,3)$ are the unit and Pauli matrices in the spin and Nambu spaces, respectively. $\boldsymbol{\sigma}=(\sigma_1,\sigma_2,\sigma_3)$ is the vector of Pauli matrices.

The Usadel equation in the N in this rotating frame has the form[16,24,25]

$$D\boldsymbol{\nabla}(\hat{g}\boldsymbol{\nabla}\hat{g})+[i\varepsilon\tau_3+i(\Omega/2)\sigma_3\otimes\tau_3,\hat{g}]=0, \tag{4}$$

where D is the diffusion constant and ε is the quasiparticle energy measured from the Fermi level. See Appendix A for the derivation. To take into account the magnetic proximity effect, we consider a low-transparency spin-active interface at the F/N contact, with the boundary condition on the N side given by[14,26]

$$2\gamma_B\xi\hat{g}\partial_x\hat{g}=[\tau_3+i\gamma_\phi(\mathbf{m}\cdot\boldsymbol{\sigma})\otimes\tau_3,\hat{g}]. \tag{5}$$

Here, $\gamma_B=R_bL/R_d\xi$ and $\gamma_\phi=G_\phi/G_T$, in terms of the interfacial resistance parameter R_b, the diffusive resistance of the N R_d, the N coherence length ξ, the imaginary part of the mixing conductance[27] G_ϕ, and the interfacial tunneling conductance $G_T=1/R_b$. The mixing conductance describes the spin rotation in the plane perpendicular to the magnetization axis upon interfacial reflection. The magnetic proximity effect is governed by γ_ϕ.[14] We will for simplicity disregard the real part of the mixing conductance and the spin dependence of the F/N conductance, which should not affect our findings qualitatively. We make use of the well-known Kupriyanov-Lukichev boundary conditions[28] for the N/S interface

$$-2\gamma_B\xi\hat{g}\partial_x\hat{g}=[\hat{g}_S,\hat{g}] \tag{6}$$

with the bulk Green's functions $\hat{g}_S$. For simplicity, we assume the same γ_B parameter at both interfaces.

Focusing on the tunneling regime with weak superconducting correlations in N, we linearize the Usadel equation with respect to the anomalous Green's function in the N. The linearized Usadel equation reads

$$D\partial_x^2 f_s+2i\varepsilon f_s-2i\mathbf{f}_t\cdot\mathbf{h}=0,$$

$$D\partial_x^2\mathbf{f}_t+2i\varepsilon\mathbf{f}_t-2if_s\mathbf{h}=0 \tag{7}$$

with $\mathbf{h}=-\Omega\mathbf{z}/2$ and $\mathbf{z}=(0,0,1)$. The general solution in the N is thus

$$\begin{pmatrix} f_s \\ \mathbf{f}_t \end{pmatrix}\equiv\begin{pmatrix} f_s \\ f_1 \\ 0 \\ f_3 \end{pmatrix}=(Ae^{ik_+x}+A'e^{-ik_+x})\begin{pmatrix} 1 \\ 0 \\ 0 \\ -1 \end{pmatrix}+(Be^{ik_-x}+B'e^{-ik_-x})\begin{pmatrix} 1 \\ 0 \\ 0 \\ 1 \end{pmatrix}+(Ce^{ik_0x}+C'e^{-ik_0x})\begin{pmatrix} 0 \\ 1 \\ 0 \\ 0 \end{pmatrix} \tag{8}$$

with $k_\pm=\sqrt{2i(-\varepsilon\pm\Omega/2)/D}$ and $k_0=\sqrt{-2i\varepsilon/D}$. The coefficients A,A',B,B',C and C' are determined by the boundary conditions. Here, f_1 is the transverse triplet component, which is long ranged at low energies, and f_3 is the longitudinal triplet component, which is short ranged, similarly to the singlet component f_s.[6] It follows from the boundary conditions that the second component of $\mathbf{f}_t$ is zero.

Linearizing the boundary conditions at the N/F interface, we have

$$\gamma_B\xi\partial_x f_s=f_s+i\gamma_\phi\mathbf{f}_t\cdot\mathbf{m},$$

$$\gamma_B\xi\partial_x\mathbf{f}_t=\mathbf{f}_t+i\gamma_\phi f_s\mathbf{m}. \tag{9}$$

These boundary conditions show that the presence of f_s generates the triplet components with $\mathbf{f}_t\|\mathbf{m}$ as long as $\gamma_\phi\neq0$. Similarly, the linearized boundary conditions at the N/S interface have the form

$$\gamma_B\xi\partial_x f_s+g_S^0f_s+g_S^3f_3=f_S^0,$$

$$\gamma_B\xi\partial_x\mathbf{f}_t+g_S^0\mathbf{f}_t+g_S^3f_s\mathbf{z}=f_S^3\mathbf{z}. \tag{10}$$

Here, the bulk Green's functions in the S, g_S and f_S, are given by $g_S=(g_S^0\sigma_0+g_S^3\sigma_3)\otimes\tau_3$ and $f_S=(f_S^0\sigma_0+f_S^3\sigma_3)\otimes\tau_1$, where (in a convenient gauge)

$$g_S^0=\frac{1}{2}\left(\frac{-i(\varepsilon+\Omega/2)}{\sqrt{\Delta^2-(\varepsilon+\Omega/2)^2}}+\frac{-i(\varepsilon-\Omega/2)}{\sqrt{\Delta^2-(\varepsilon-\Omega/2)^2}}\right),$$

$$g_S^3=\frac{1}{2}\left(\frac{-i(\varepsilon+\Omega/2)}{\sqrt{\Delta^2-(\varepsilon+\Omega/2)^2}}-\frac{-i(\varepsilon-\Omega/2)}{\sqrt{\Delta^2-(\varepsilon-\Omega/2)^2}}\right),$$

$$f_S^0=\frac{1}{2}\left(\frac{\Delta}{\sqrt{\Delta^2-(\varepsilon+\Omega/2)^2}}+\frac{\Delta}{\sqrt{\Delta^2-(\varepsilon-\Omega/2)^2}}\right),$$

$$f_S^3=\frac{1}{2}\left(\frac{\Delta}{\sqrt{\Delta^2-(\varepsilon+\Omega/2)^2}}-\frac{\Delta}{\sqrt{\Delta^2-(\varepsilon-\Omega/2)^2}}\right). \tag{11}$$

After the unilluminating manipulations to solve Eqs. (8)–(10), we obtain the desired solution of the Usadel equation. The explicit form of the solution is rather complicated and is given in Appendix B.

In general, the tilt angle θ is determined by solving the Landau-Lifshitz-Gilbert equation

$$\frac{d\mathbf{m}(t)}{dt} = -\gamma \mathbf{m}(t) \times \mathbf{H}_{\text{eff}}(t) + \alpha \mathbf{m}(t) \times \frac{d\mathbf{m}(t)}{dt}, \quad (12)$$

where γ is the gyromagnetic ratio, $\mathbf{H}_{\text{eff}}$ is the effective magnetic field, and α is the Gilbert damping constant. Driving the ferromagnet by an applied transverse rotating magnetic field h_{rf}, in the presence of an effective static dc field H_{dc}, we find a small transverse magnetic field in the rotating frame of reference. This is disregarded in our analysis, assuming $\alpha \ll 1$, so that $\theta \sim h_{\text{rf}}/\alpha H_{\text{dc}} \gg h_{\text{rf}}/H_{\text{dc}}$ at the ferromagnetic resonance, which is usually the case in realistic ferromagnets. We consider H_{dc} due to the internal demagnetization and crystalline anisotropy fields in the F. Then, the effective magnetic field can be neglected outside of the F. However, even if we take into account some H_{dc} outside of the F, our key findings do not change qualitatively. We can also envision exciting and tuning ferromagnetic resonance by spin torques (see, e.g., Ref. 29) as well as controlling the resonance frequency Ω by the microwave power rather than H_{dc}.

We note that the spin-pumping effect is enhanced close to the ferromagnetic resonance, which should in practice be the optimal driving regime for the magnetic dynamics. Notice also that the tilt angle of the rotating magnetization θ may in general be time dependent. In this paper, we focus on the regime when $d \ln \theta/dt \ll (\Omega, \theta^2/\tau_i)$ so that the appropriate nonequilibrium spin state is fully developed before θ changes appreciably. Here, $1/\tau_i$ is an effective spin-injection rate proportional to the mixing conductance at the F/N interface.[30] In addition, the spin-relaxation rate is assumed to satisfy $1/\tau_{\text{sf}} \ll \Omega$ so that the spin memory is preserved during a cycle of precession and $1/\tau_{\text{sf}} \ll \theta^2/\tau_i$ so that the developed spin accumulation does not decay. We will, therefore, fix θ and disregard spin relaxation in the junction in the following.

Next, let us consider tunneling current between the N and the STM tip. See Fig. 1. Below, we consider two cases: spin relaxation in the STM tip is weak or strong, on the scale of its characteristic spin-injection rate. Weak (strong) spin relaxation effectively leads to a state of equilibrium in the STM tip, in the rotating (laboratory) frame of reference. To realize the situation that the state of equilibrium is effectively reached in the rotating frame of reference, the STM tip should be spin-polarized by the fictitious field, which would in practice require either connecting the precessing ferromagnet directly to the tip or using magnetized tip which itself is precessing in synchronization. Experimentally, this may be more difficult to realize than the strong spin-relaxation regime in the STM tip. (Note, however, that a spin-resolved STM technique has been recently developed.[31]) One may furthermore think that the limit when $\Omega \sim \Delta$ is problematic for the superconductor since the gap should then be strongly suppressed. However, assuming some spin relaxation in S, the out-of-equilibrium pumped spins do not cause significant Cooper-pair depairing in the superconductor while the effective spin relaxation in N is weak so that the pumped spin distribution is unaffected in N.

Now, let us first consider the case of the STM tip with weak spin relaxation. We define the 8×8 matrix Green's functions in STM and N, $\check{g}_{\text{STM}}$ and $\check{g}_{\text{N}}$, as

$$\check{g}_{\text{STM}} = \begin{pmatrix} \tau_3 & \hat{g}^K_{\text{STM}} \\ 0 & -\tau_3 \end{pmatrix}, \quad \check{g}_{\text{N}} = \begin{pmatrix} \hat{g}^R_{\text{N}} & \hat{g}^K_{\text{N}} \\ 0 & \hat{g}^A_{\text{N}} \end{pmatrix}. \quad (13)$$

Here, R, K and A represent the retarded, Keldysh and advanced components, respectively. The current between the N and the STM tip is given by

$$I \sim \int d\varepsilon \, \text{Tr}(\tau_3 [\check{g}_{\text{STM}}, \check{g}_{\text{N}}]^K), \quad (14)$$

where

$$[\check{g}_{\text{STM}}, \check{g}_{\text{N}}]^K = \hat{g}^K_{\text{STM}} \hat{g}^A_{\text{N}} - \hat{g}^R_{\text{N}} \hat{g}^K_{\text{STM}} + \tau_3 \hat{g}^K_{\text{N}} + \hat{g}^K_{\text{N}} \tau_3. \quad (15)$$

Let us apply a bias voltage V to the STM tip so that we have

$$\begin{aligned} \hat{g}^K_{\text{STM}} &= \tau_3 (f^0_{\text{STM}} + f^3_{\text{STM}} \tau_3) + (f^0_{\text{STM}} + f^3_{\text{STM}} \tau_3) \tau_3 \\ &= 2 f^3_{\text{STM}} + 2 f^0_{\text{STM}} \tau_3, \end{aligned}$$

$$\begin{aligned} f^{0(3)}_{\text{STM},\sigma} = [&\tanh\{(\varepsilon + eV + \sigma\Omega/2)/2T\} + (-)\tanh\{(\varepsilon - eV \\ &- \sigma\Omega/2)/2T\}]/2 \end{aligned} \quad (16)$$

with $\sigma = \pm$ for spins up and down, and $\hat{g}^K_{\text{N}} = \tanh(\varepsilon/2T)(\hat{g}^R_{\text{N}} - \hat{g}^A_{\text{N}})$. Therefore, we obtain

$$\begin{aligned} \text{Tr}(\tau_3 [g_{\text{STM}}, g_{\text{N}}]^K) &= \sum_\sigma 2 f^3_{\text{STM},\sigma} (g^A_{\text{N},\sigma} - g^R_{\text{N},\sigma}) \\ &= -\sum_\sigma 4 f^3_{\text{STM},\sigma} \, \text{Re} \, g^R_{\text{N},\sigma}, \end{aligned} \quad (17)$$

and, hence, at zero temperature

$$dI/dV \sim \sum_\sigma [N_\sigma(-eV - \sigma\Omega/2) + N_\sigma(eV + \sigma\Omega/2)]. \quad (18)$$

Here, $N_\sigma = \text{Re} \, g^R_{N,\sigma}$ denotes the density of states for spin σ in the N. To calculate the spin-resolved density of states N_σ, we can use the relation $\mathbf{g} = -f_s \mathbf{f}_t$, which is obtained from the normalization condition $\hat{g}^2 = 1$ applied to the parametrization Eq. (3).

In the case of the STM tip with weak spin relaxation, the state in the STM is equilibrated in the rotating frame of reference and we obtain the relevant results by setting $\Omega = 0$ in Eqs. (16) and (18). The tunneling conductance then coincides exactly with the density of states.

III. RESULTS

In the numerical calculations, we introduce a small imaginary part of the energy, $\varepsilon \to \varepsilon + i\delta$, to regularize singularities. Physically, δ captures an effective depairing rate for Cooper pairs. We choose the following parameters: $\gamma_B = 100$, $\theta = \pi/12$, $L/\xi = 10$, $\Delta/E_{\text{Th}} = 0.1$, and $\delta/E_{\text{Th}} = 0.01$. Here, $E_{\text{Th}} = D/L^2$ is the Thouless energy. Typically, for $L/\xi = 10$ and $E_{\text{Th}} \sim 0.01$ meV.

A. Weak spin relaxation in the STM tip

We start by considering the case of weak spin relaxation in the STM tip. We first discuss some limiting cases and give qualitative picture of our main results. Below, we focus on

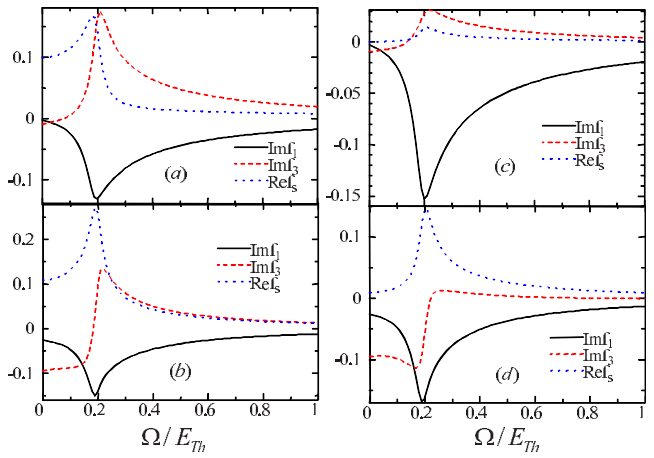

FIG. 2. (Color online) Anomalous Green's functions as a function of Ω/E_{Th} at the N/S interface ($x=L$) with (a) $\gamma_\phi=100$ and (b) $\gamma_\phi=10$ and at the F/N interface ($x=0$) with (c) $\gamma_\phi=100$ and (d) $\gamma_\phi=10$. Here, we set $\varepsilon=0$. f_1 and f_3 are the odd-frequency and f_s is the even-frequency pairing amplitudes.

the low-energy limit, i.e., $\varepsilon\to 0$, where the superconductivity is manifested most strongly. At $\varepsilon=0$, the bulk Green's functions in the S are given by

$$g_S^0=0,\quad g_S^3=\frac{-i\Omega/2}{\sqrt{\Delta^2-(\Omega/2)^2}},\tag{19}$$

$$f_S^0=\frac{\Delta}{\sqrt{\Delta^2-(\Omega/2)^2}},\quad f_S^3=0,\tag{20}$$

for $\Omega<2\Delta$ and

$$g_S^0=\frac{\Omega/2}{\sqrt{(\Omega/2)^2-\Delta^2}},\quad g_S^3=0,\tag{21}$$

$$f_S^0=0,\quad f_S^3=\frac{i\Delta}{\sqrt{(\Omega/2)^2-\Delta^2}},\tag{22}$$

for $\Omega>2\Delta$. In the limit of $\Omega\to 2\Delta$, these Green's functions diverge and the proximity effect is resonantly enhanced as seen from the boundary conditions at the N/S interfaces. Taking the limit $\gamma_\phi\to\infty$ for the boundary condition at the F/N interface, we have $f_s\to 0$ and $f_1 \sin\theta+f_3\cos\theta\to 0$. The singlet component vanishes while the triplet components can remain finite for $\theta\neq 0,\ \pi/2$ in this limit. Thus, we can expect that by tuning Ω close to 2Δ one can control the magnitude of the odd-frequency superconductivity for sufficiently large γ_ϕ.

Next, let us plot the anomalous Green's functions using Eq. (8). Figure 2 shows anomalous Green's functions at the N/S interface ($x=L$) as a function of Ω/E_{Th} with (a) $\gamma_\phi=100$ and (b) $\gamma_\phi=10$. Note that at $\varepsilon=0$, f_1 and f_3 are purely imaginary while f_s is a real number. We find that a resonant peak appears at $\Omega=2\Delta$. As seen in Fig. 2(a), for $\Omega<2\Delta$, the singlet component dominates, while, for $\Omega>2\Delta$, the triplet component dominates. This can be understood by the fact that for $\Omega\to 2\Delta-0^+$, f_S^0 diverges while for $\Omega\to 2\Delta+0^+$, f_S^3 diverges. *Thus, one can control a crossover from the dominant even to the dominant odd-frequency superconductivity by changing* Ω, which is tunable by the external magnetic field. When γ_ϕ is reduced, the singlet component is enhanced as shown in Fig. 2(b). We also show the anomalous Green's functions at the F/N interface ($x=0$) as a function of Ω/E_{Th} in Fig. 2(c) for $\gamma_\phi=100$ and Fig. 2(d) for $\gamma_\phi=10$. A peak also appears at $\Omega=2\Delta$. Compared to the results at $x=L$, the long-range triplet component f_1 has a large magnitude, which is controllable by tuning the frequency Ω.

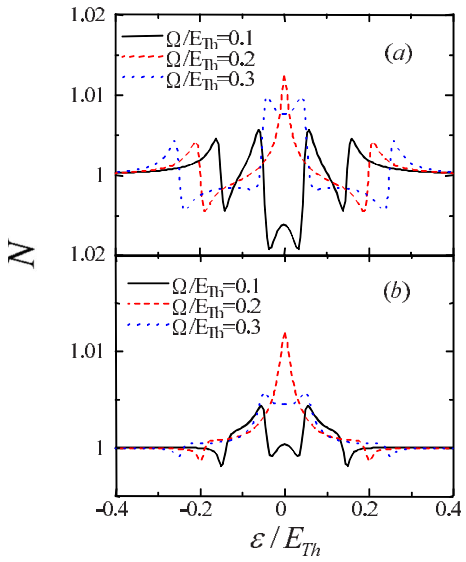

FIG. 3. (Color online) The density of states normalized by its normal-state value as a function of $\varepsilon/E_{\mathrm{Th}}$ with $\gamma_\phi=100$ at (a) $x=L$ and (b) $x=0$.

To date, a hallmark of the odd-frequency pairing has been considered to be the long-ranged proximity effect in the presence of magnetism.[6] However, another aspect of this pairing has been recently appreciated: The density of states in the presence of the odd-frequency pairing is enhanced, acquiring a zero-energy peak within the gap structure.[8,21,32,33] Using general relations for the conjugate Green's functions,[34] we have that $\tilde{f}_s(\varepsilon)=f_s^*(-\varepsilon)$ and $\tilde{\mathbf{f}}_t(\varepsilon)=-\mathbf{f}_t^*(-\varepsilon)$. Hence, we easily obtain $g^2=1-|f_s(0)|^2+|\mathbf{f}_t(0)|^2$ at $\varepsilon=0$, from the standard normalization condition $\hat{g}^2=1$. Therefore, the density of states, which is given by $\mathrm{Re}\, g$, is enhanced by the generation of odd-frequency pairing ($\mathbf{f}_t$) and suppressed by the presence of the even-frequency pairing (f_s) at $\varepsilon=0$.

The density of states normalized by its normal-state value, $N=\mathrm{Re}\sqrt{1-(f_s^2+f_1^2+f_3^2)}$, as a function of $\varepsilon/E_{\mathrm{Th}}$ is shown in Fig. 3 setting $\gamma_\phi=100$ at (a) $x=L$ and (b) $x=0$. We find a crossover from the gap to the peak structure in the density of states with increasing Ω/E_{Th}. This reflects a crossover from the dominant even to the dominant odd-frequency superconductivity in the N, upon changing the precessional frequency. Note that, as shown above, the density of states exactly coincides with the tunneling conductance between the N and the STM tip, in the weak spin-relaxation regime of the STM tip.

B. Strong spin relaxation in the STM tip

Here, we discuss the more realistic case with strong spin relaxation in the STM tip so that the tip is equilibrated in the

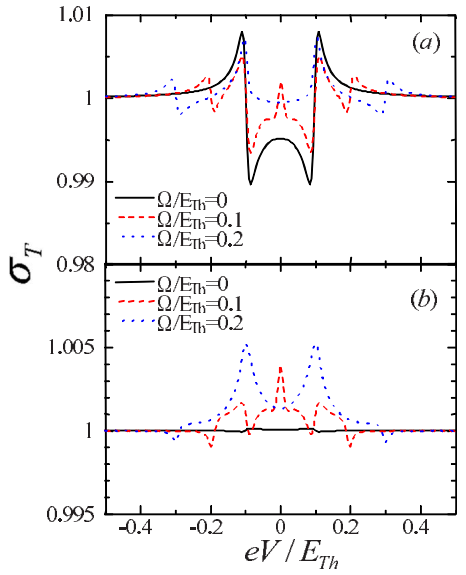

FIG. 4. (Color online) The normalized tunneling conductance as a function of eV/E_{Th} with $\gamma_\phi=100$ at (a) $x=L$ and (b) $x=0$.

laboratory frame. Let us define σ_T as dI/dV normalized by its normal-state value. Figure 4 shows σ_T as a function of eV/E_{Th} for $\gamma_\phi=100$ at (a) $x=L$ and (b) $x=0$. We see the gap structure at $\Omega=0$. For larger Ω, the zero-bias conductance grows and a sharp zero-bias peak emerges at $\Omega/E_{\mathrm{Th}}=0.1$. This can be understood as follows: let us consider the term $N_\uparrow(eV+\Omega/2)$ in Eq. (18), for instance. Then, the argument $\varepsilon-\Omega/2$ appearing in Eqs. (4) and (11) is effectively replaced by eV while $\varepsilon+\Omega/2$ is replaced by $\mathrm{eV}+\Omega$. Similar replacements should be made for other terms in Eq. (18). Thus, coherence peaks will appear at $\mathrm{eV}=\Omega\pm\Delta$. Therefore, when $\Omega=\Delta$, a resonant peak appears at the zero bias. This can be also attributed to the emergence of the odd-frequency pairing, as shown in Sec. III A. Therefore, we find that even in the case of the strong spin relaxation in the STM, we can also find the evidence of the odd triplet superconductivity (zero-bias peak) tuned by the precession frequency.

IV. CONCLUSIONS

We have studied the proximity effect in diffusive F/N/S junctions with precessing magnetization of the F layer. We found that a tunable odd-frequency pairing in the N is governed by spin correlations in the N that are induced by the ferromagnetic precession. At the resonance frequency, $\Omega\rightarrow 2\Delta$, the odd-frequency pairing is strongly enhanced. We unveiled that the odd-frequency pairing can be dominant over the even-frequency pairing in the N by tuning the precessional frequency. This is manifested as the crossover from the gap to the peak structure in the tunneling conductance between the N and the STM tip, where we investigated two regimes of the weak and strong spin relaxation in the STM tip.

Our results can be experimentally accessible and provide a way to amplify the odd triplet superconductivity using the magnetization precession in the F/N/S junctions. These characteristics should be observable by a scanning-tunneling microscope or other tunneling experiments and, hence, may serve as a smoking gun to reveal the odd-frequency superconductivity.

In the tunneling experiment in PdNi/Nb junctions, the crossover from the gap to the peak structure in the tunneling conductance has been found.[35] This would also reflect the pairing symmetry in the ferromagnetic layer. In this experiment, this crossover has been observed by using several samples with different thickness of the ferromagnet. Our proposal given in the present paper is experimentally easier since it can be tested with one sample.

Recently, the F/N/S trilayer junctions have been fabricated to study behavior of the superconducting phase transition.[36,37] Also, a ferromagnetic resonance experiment has been performed in an Nb/permalloy proximity system.[38] In the light of these advances, it appears realistic to verify our predictions experimentally by using, e.g., permalloy/Cu/Nb junctions. The predicted resonance frequency corresponds to the ~MHz range and is easily achievable by the present-day experimental technique. It should be remarked, however, that the required condition for the spin-flip relaxation rate, $1/\tau_{\mathrm{sf}}\ll\Omega$, is rather stringent in this low-frequency limit, requiring low temperatures.

ACKNOWLEDGMENTS

We are grateful to A. Brataas, Ya. V. Fominov, M. Houzet, J. Linder, and J. Inoue for helpful discussions. This work was supported by the JSPS (T.Y.) and by the Alfred P. Sloan Foundation (Y.T.).

APPENDIX A: DERIVATION OF THE USADEL EQUATION

Here, we present the derivation of the Usadel equation in the presence of the effective Zeeman field. The matrix Green's function in particle-hole ⊗ spin space can be defined as[6]

$$\hat{G}=-i\begin{pmatrix}\langle T_C a_\uparrow a_\uparrow^\dagger\rangle & \langle T_C a_\uparrow a_\downarrow^\dagger\rangle & \langle T_C a_\uparrow a_\downarrow\rangle & \langle T_C a_\uparrow a_\uparrow\rangle\\ \langle T_C a_\downarrow a_\uparrow^\dagger\rangle & \langle T_C a_\downarrow a_\downarrow^\dagger\rangle & \langle T_C a_\downarrow a_\downarrow\rangle & \langle T_C a_\downarrow a_\uparrow\rangle\\ \langle T_C a_\downarrow^\dagger a_\uparrow^\dagger\rangle & \langle T_C a_\downarrow^\dagger a_\downarrow^\dagger\rangle & \langle T_C a_\downarrow^\dagger a_\downarrow\rangle & \langle T_C a_\downarrow^\dagger a_\uparrow\rangle\\ \langle T_C a_\uparrow^\dagger a_\uparrow^\dagger\rangle & \langle T_C a_\uparrow^\dagger a_\downarrow^\dagger\rangle & \langle T_C a_\uparrow^\dagger a_\downarrow\rangle & \langle T_C a_\uparrow^\dagger a_\uparrow\rangle\end{pmatrix}, \tag{A1}$$

where T_C is the time-ordering operator along the Keldysh time contour. This basis is obtained from the conventional basis

$$\hat{G}=-i\begin{pmatrix}\langle T_C a_\uparrow a_\uparrow^\dagger\rangle & \langle T_C a_\uparrow a_\downarrow^\dagger\rangle & \langle T_C a_\uparrow a_\uparrow\rangle & \langle T_C a_\uparrow a_\downarrow\rangle\\ \langle T_C a_\downarrow a_\uparrow^\dagger\rangle & \langle T_C a_\downarrow a_\downarrow^\dagger\rangle & \langle T_C a_\downarrow a_\uparrow\rangle & \langle T_C a_\downarrow a_\downarrow\rangle\\ \langle T_C a_\uparrow^\dagger a_\uparrow^\dagger\rangle & \langle T_C a_\uparrow^\dagger a_\downarrow^\dagger\rangle & \langle T_C a_\uparrow^\dagger a_\uparrow\rangle & \langle T_C a_\uparrow^\dagger a_\downarrow\rangle\\ \langle T_C a_\downarrow^\dagger a_\uparrow^\dagger\rangle & \langle T_C a_\downarrow^\dagger a_\downarrow^\dagger\rangle & \langle T_C a_\downarrow^\dagger a_\uparrow\rangle & \langle T_C a_\downarrow^\dagger a_\downarrow\rangle\end{pmatrix}, \tag{A2}$$

by the following transformation

$$\hat{G}\rightarrow U\hat{G}U^\dagger \tag{A3}$$

with

$$\hat{U} = \begin{pmatrix} 1 & 0 \\ 0 & \sigma_1 \end{pmatrix}. \tag{A4}$$

With the quasiclassical approximation, we obtain the quasiclassical Green's function $\hat{g}$ from $\hat{G}$ in this basis.[6]

Then, the pair potential is transformed as

$$\hat{\Delta} = \begin{pmatrix} 0 & \Delta\sigma_2 \\ \Delta^*\sigma_2 & 0 \end{pmatrix} = (\tau_1 \,\mathrm{Re}\,\Delta - \tau_2 \,\mathrm{Im}\,\Delta) \otimes \sigma_2, \tag{A5}$$

$$\rightarrow \begin{pmatrix} 0 & \Delta\sigma_2\sigma_1 \\ \Delta^*\sigma_1\sigma_2 & 0 \end{pmatrix} = \begin{pmatrix} 0 & -i\Delta\sigma_3 \\ i\Delta^*\sigma_3 & 0 \end{pmatrix} = (\tau_2 \,\mathrm{Re}\,\Delta + \tau_1 \,\mathrm{Im}\,\Delta) \otimes \sigma_3 \tag{A6}$$

and also we have

$$\hat{\boldsymbol{\sigma}} = \begin{pmatrix} \boldsymbol{\sigma} & 0 \\ 0 & \boldsymbol{\sigma}^* \end{pmatrix} \rightarrow \begin{pmatrix} \boldsymbol{\sigma} & 0 \\ 0 & \sigma_1\boldsymbol{\sigma}^*\sigma_1 \end{pmatrix} = (\tau_0 \otimes \sigma_1, \tau_0 \otimes \sigma_2, \tau_3 \otimes \sigma_3) \equiv \hat{\boldsymbol{S}}. \tag{A7}$$

The Usadel equation is, therefore, transformed by $\hat{U}$ as[6]

$$D\boldsymbol{\nabla}(\hat{g}\boldsymbol{\nabla}\hat{g}) + [i\varepsilon\tau_3 - i(\mathbf{h}\cdot\hat{\boldsymbol{\sigma}}) - (\tau_1 \,\mathrm{Re}\,\Delta - \tau_2 \,\mathrm{Im}\,\Delta) \otimes \sigma_2, \hat{g}] = 0, \tag{A8}$$

$$\rightarrow D\boldsymbol{\nabla}(\hat{g}\boldsymbol{\nabla}\hat{g}) + [i\varepsilon\tau_3 - i(\mathbf{h}\cdot\hat{\boldsymbol{S}}) - (\tau_2 \,\mathrm{Re}\,\Delta + \tau_1 \,\mathrm{Im}\,\Delta) \otimes \sigma_3, \hat{g}] = 0. \tag{A9}$$

Next, we consider the following unitary transformation:[25]

$$V = \exp\left[i\frac{\pi}{4}\tau_3 \otimes \sigma_3\right]\exp\left[-i\frac{\pi}{4}\sigma_3\right], \tag{A10}$$

such that

$$V\sigma_1 V^\dagger = \sigma_1 \otimes \tau_3, \quad V\sigma_2 V^\dagger = \sigma_2 \otimes \tau_3,$$

$$V\tau_2 \otimes \sigma_3 V^\dagger = \tau_1, \quad V\tau_1 \otimes \sigma_3 V^\dagger = -\tau_2 \tag{A11}$$

employing the relation

$$e^{i\theta\mathbf{n}\cdot\boldsymbol{\sigma}} = \cos\theta + i\sin\theta\mathbf{n}\cdot\boldsymbol{\sigma} \tag{A12}$$

for an arbitrary unit vector $\mathbf{n}$. The Usadel equation is finally transformed by V as[25]

$$D\boldsymbol{\nabla}(\hat{g}\boldsymbol{\nabla}\hat{g}) + [i\varepsilon\tau_3 - i(\mathbf{h}\cdot\hat{\boldsymbol{S}}) - (\tau_2 \,\mathrm{Re}\,\Delta + \tau_1 \,\mathrm{Im}\,\Delta) \otimes \sigma_3, \hat{g}] = 0, \tag{A13}$$

$$\rightarrow D\boldsymbol{\nabla}(\hat{g}\boldsymbol{\nabla}\hat{g}) + [i\varepsilon\tau_3 - i(\mathbf{h}\cdot\boldsymbol{\sigma}) \otimes \tau_3 - (\tau_1 \,\mathrm{Re}\,\Delta - \tau_2 \,\mathrm{Im}\,\Delta) \otimes \sigma_0, \hat{g}] = 0. \tag{A14}$$

This representation of the Usadel equation for the transformed Green's function has the convenience of the explicit symmetry with respect to rotations of the effective Zeeman field $\mathbf{h}$.

Assuming that Δ is real, the equation for the f component yields

$$D\boldsymbol{\nabla}(g\boldsymbol{\nabla}f + f\boldsymbol{\nabla}\tilde{g}) + 2i\varepsilon f - i(f\mathbf{h}\cdot\boldsymbol{\sigma} + \mathbf{h}\cdot\boldsymbol{\sigma}f) = \Delta\tilde{g} - \Delta g. \tag{A15}$$

Linearizing this equation with respect to superconducting correlations, we find

$$D\boldsymbol{\nabla}^2 f + 2i\varepsilon f - i(fh\cdot\boldsymbol{\sigma} + \mathbf{h}\cdot\boldsymbol{\sigma}f) = -2\Delta. \tag{A16}$$

Setting $f = f_s + \mathbf{f}_t\cdot\boldsymbol{\sigma}$,[23] we have

$$D\boldsymbol{\nabla}^2(f_s + \mathbf{f}_t\cdot\boldsymbol{\sigma}) + 2i\varepsilon(f_s + \mathbf{f}_t\cdot\boldsymbol{\sigma}) - i(2f_s\mathbf{h}\cdot\boldsymbol{\sigma} + 2\mathbf{f}_t\cdot\mathbf{h}) = -2\Delta, \tag{A17}$$

giving finally

$$D\boldsymbol{\nabla}^2 f_s + 2i\varepsilon f_s - 2i\mathbf{f}_t\cdot\mathbf{h} = -2\Delta, \tag{A18}$$

$$D\boldsymbol{\nabla}^2\mathbf{f}_t + 2i\varepsilon\mathbf{f}_t - 2if_s\mathbf{h} = 0. \tag{A19}$$

Here, $\mathbf{f}_t$ and $\mathbf{h}$ are three-dimensional vectors. As shown in Ref. 23, f_s and $\mathbf{f}_t \| \mathbf{h}$ are short ranged while $\mathbf{f}_t \perp \mathbf{h}$ is long ranged, at low energies.

APPENDIX B: SOLUTION OF THE USADEL EQUATION

Solving Eqs. (8)–(10), we obtain the solution of the Usadel equation as follows:

$$C = \frac{-a_3a_4a_7 - a_1a_6a_8 + a_1a_4a_{10}}{a_2a_4a_7 + a_1a_5a_8 - a_1a_4a_9},$$

$$A = -(a_2C + a_3)/a_1, \quad B = -(a_5C + a_6)/a_4, \quad A' = b_1A + b_2,$$

$$B' = b_3B + b_4, \quad \text{and} \quad C' = b_5C, \quad \text{where}$$

$$a_1 = 1 - i\gamma_B\xi k_+ - i\gamma_\phi\cos\theta + (1 + i\gamma_B\xi k_+ - i\gamma_\phi\cos\theta)b_1,$$

$$a_2 = i\gamma_\phi(1 + b_5)\sin\theta/2,$$

$$a_3 = (1 + i\gamma_B\xi k_+ - i\gamma_\phi\cos\theta)b_2,$$

$$a_4 = 1 - i\gamma_B\xi k_- + i\gamma_\phi\cos\theta + (1 + i\gamma_B\xi k_- + i\gamma_\phi\cos\theta)b_3,$$

$$a_5 = i\gamma_\phi(1 + b_5)\sin\theta/2,$$

$$a_6 = (1 + i\gamma_B\xi k_- + i\gamma_\phi\cos\theta)b_4,$$

$$a_7 = i\gamma_\phi\sin\theta(1 + b_1),$$

$$a_8 = i\gamma_\phi\sin\theta(1 + b_3),$$

$$a_9 = 1 - i\gamma_B\xi k_0 + (1 + i\gamma_B\xi k_0)b_5,$$

$$a_{10} = i\gamma_\phi\sin\theta(b_2 + b_4) \tag{B1}$$

and

$$b_1 = -\frac{g_S^0 - g_S^3 + i\gamma_B\xi k_+}{g_S^0 - g_S^3 - i\gamma_B\xi k_+}e^{2ik_+L},$$

$$b_2 = \frac{e^{ik_+L} f_S^-}{g_S^0 - g_S^3 - i\gamma_B \xi k_+},$$

$$b_3 = -\frac{g_S^0 + g_S^3 + i\gamma_B \xi k_-}{g_S^0 + g_S^3 - i\gamma_B \xi k_-} e^{2ik_-L},$$

$$b_4 = \frac{e^{ik_-L} f_S^+}{g_S^0 + g_S^3 - i\gamma_B \xi k_-},$$

$$b_5 = -\frac{g_S^0 + i\gamma_B \xi k_0}{g_S^0 - i\gamma_B \xi k_0} e^{2ik_0L},$$

with $f_S^{\pm} = (f_S^0 \pm f_S^3)/2$.

[1] V. L. Berezinskii, JETP Lett. **20**, 287 (1974).

[2] A. Balatsky and E. Abrahams, Phys. Rev. B **45**, 13125 (1992); E. Abrahams, A. Balatsky, D. J. Scalapino, and J. R. Schrieffer, *ibid.* **52**, 1271 (1995).

[3] P. Coleman, E. Miranda, and A. Tsvelik, Phys. Rev. Lett. **70**, 2960 (1993); Phys. Rev. B **49**, 8955 (1994); Phys. Rev. Lett. **74**, 1653 (1995).

[4] M. Vojta and E. Dagotto, Phys. Rev. B **59**, R713 (1999).

[5] Y. Fuseya, H. Kohno, and K. Miyake, J. Phys. Soc. Jpn. **72**, 2914 (2003).

[6] F. S. Bergeret, A. F. Volkov, and K. B. Efetov, Phys. Rev. Lett. **86**, 4096 (2001); A. F. Volkov, F. S. Bergeret, and K. B. Efetov, *ibid.* **90**, 117006 (2003); F. S. Bergeret, A. F. Volkov, and K. B. Efetov, Rev. Mod. Phys. **77**, 1321 (2005).

[7] A. Kadigrobov, R. I. Shekter, and M. Jonson, Europhys. Lett. **54**, 394 (2001).

[8] Y. Tanaka and A. A. Golubov, Phys. Rev. Lett. **98**, 037003 (2007).

[9] Y. Tanaka, A. A. Golubov, S. Kashiwaya, and M. Ueda, Phys. Rev. Lett. **99**, 037005 (2007).

[10] M. Eschrig, T. Löfwander, Th. Champel, J. C. Cuevas, and G. Schön, J. Low Temp. Phys. **147**, 457 (2007).

[11] M. Eschrig and T. Löfwander, Nat. Phys. **4**, 138 (2008).

[12] T. Yokoyama, Y. Tanaka, and A. A. Golubov, Phys. Rev. B **78**, 012508 (2008); T. Yokoyama, M. Ichioka, and Y. Tanaka, arXiv:0904.2961 (unpublished).

[13] J. Linder, T. Yokoyama, A. Sudbø, and M. Eschrig, Phys. Rev. Lett. **102**, 107008 (2009); J. Linder, T. Yokoyama, and A. Sudbø, Phys. Rev. B **79**, 054523 (2009).

[14] D. Huertas-Hernando, Yu. V. Nazarov, and W. Belzig, arXiv:cond-mat/0204116 (unpublished); Phys. Rev. Lett. **88**, 047003 (2002); D. Huertas-Hernando and Yu. V. Nazarov, Eur. Phys. J. B **44**, 373 (2005).

[15] S. Takahashi, S. Hikino, M. Mori, J. Martinek, and S. Maekawa, Phys. Rev. Lett. **99**, 057003 (2007); S. Hikino, M. Mori, S. Takahashi, and S. Maekawa, J. Phys. Soc. Jpn. **77**, 053707 (2008).

[16] M. Houzet, Phys. Rev. Lett. **101**, 057009 (2008).

[17] F. Konschelle and A. Buzdin, Phys. Rev. Lett. **102**, 017001 (2009).

[18] R. S. Keizer, S. T. B. Goennenwein, T. M. Klapwijk, G. Miao, G. Xiao, and A. Gupta, Nature (London) **439**, 825 (2006).

[19] I. Sosnin, H. Cho, V. T. Petrashov, and A. F. Volkov, Phys. Rev. Lett. **96**, 157002 (2006).

[20] Y. Tserkovnyak, A. Brataas, and G. E. W. Bauer, Phys. Rev. Lett. **88**, 117601 (2002); Phys. Rev. B **66**, 224403 (2002); Y. Tserkovnyak, A. Brataas, G. E. W. Bauer, and B. I. Halperin, Rev. Mod. Phys. **77**, 1375 (2005); Y. Tserkovnyak and A. Brataas, Phys. Rev. B **71**, 052406 (2005).

[21] V. Braude and Yu. V. Nazarov, Phys. Rev. Lett. **98**, 077003 (2007).

[22] M. Houzet and A. I. Buzdin, Phys. Rev. B **76**, 060504(R) (2007).

[23] T. Champel and M. Eschrig, Phys. Rev. B **71**, 220506(R) (2005); **72**, 054523 (2005); T. Champel, T. Löfwander, and M. Eschrig, Phys. Rev. Lett. **100**, 077003 (2008).

[24] K. D. Usadel, Phys. Rev. Lett. **25**, 507 (1970).

[25] D. A. Ivanov and Ya. V. Fominov, Phys. Rev. B **73**, 214524 (2006).

[26] A. Cottet and W. Belzig, Phys. Rev. B **72**, 180503(R) (2005).

[27] A. Brataas, Yu. V. Nazarov, and G. E. W. Bauer, Phys. Rev. Lett. **84**, 2481 (2000); Eur. Phys. J. B **22**, 99 (2001); A. Brataas, G. E. W. Bauer, and P. J. Kelly, Phys. Rep. **427**, 157 (2006).

[28] M. Yu. Kupriyanov and V. F. Lukichev, Sov. Phys. JETP **67**, 1163 (1988).

[29] A. A. Tulapurkar, Y. Suzuki, A. Fukushima, H. Kubota, H. Maehara, K. Tsunekawa, D. D. Djayaprawira, N. Watanabe, and S. Yuasa, Nature (London) **438**, 339 (2005).

[30] A. Brataas, Y. Tserkovnyak, G. E. W. Bauer, and B. I. Halperin, Phys. Rev. B **66**, 060404(R) 2002.

[31] F. Meier, L. Zhou, J. Wiebe, and R. Wiesendanger, Science **320**, 82 (2008).

[32] Y. Asano, Y. Tanaka, and A. A. Golubov, Phys. Rev. Lett. **98**, 107002 (2007); Y. Asano, Y. Sawa, Y. Tanaka, and A. A. Golubov, Phys. Rev. B **76**, 224525 (2007).

[33] T. Yokoyama, Y. Tanaka, and A. A. Golubov, Phys. Rev. B **72**, 052512 (2005); **73**, 094501 (2006); **75**, 134510 (2007).

[34] M. Eschrig, Phys. Rev. B **61**, 9061 (2000).

[35] T. Kontos, M. Aprili, J. Lesueur, and X. Grison, Phys. Rev. Lett. **86**, 304 (2001).

[36] H. Yamazaki, N. Shannon, and H. Takagi, Phys. Rev. B **73**, 094507 (2006).

[37] K. Kim and Jun Hyung Kwon, J. Kim, K. Char, H. Doh, and H. Y. Choi, Phys. Rev. B **74**, 174503 (2006).

[38] C. Bell, S. Milikisyants, M. Huber, and J. Aarts, Phys. Rev. Lett. **100**, 047002 (2008).